

## On the Impact of Thermo-mechanical Processing on Microstructure and Texture and the Resultant Anisotropy of Aluminium Sheet

Olaf Engler

Hydro Aluminium Deutschland GmbH, R&D Center Bonn, P.O. Box 2468, D – 53014 Bonn, Germany

In order to predict the mechanical properties of aluminium sheet products, the evolution of microstructure and crystallographic texture along the process chain must be tracked. During the thermo-mechanical processing in commercial production lines the material experiences a complex history of temperature, time and strain paths, which results in alternating cycles of deformation and recrystallization with the associated changes in texture and microstructure. It is demonstrated how texture control can be applied during industrial processing of Al sheet so as to improve texture-related properties of AA 3xxx AlMnMg alloys for packaging applications. Furthermore, the present paper summarizes recent developments to couple models for the simulation of changes in microchemistry, work hardening, softening, and texture evolution in order to provide for a comprehensive through-process simulation of the development of microstructure, texture and the resulting properties during the thermo-mechanical processing of Al sheet.

**Keywords:** texture, anisotropy, earing, modelling and simulation.

### 1. Introduction

During the thermo-mechanical processing of aluminium sheet products in commercial production lines the material experiences a complex history of temperature, time and strain paths, which result in alternating cycles of deformation and recrystallization with the associated changes in microstructure and crystallographic texture (Fig. 1). Thus, computer-based alloy and process development requires integration of models for simulating the evolution of microstructure, microchemistry and crystallographic texture into process models of the thermo-mechanical production of Al sheet.

In the field of Al alloys, the occurrence of plastic anisotropy of a metallic sheet constitutes one of the most prominent manifestations of crystallographic texture. For instance, when a cup is deep drawn from a circular blank cut from a textured sheet, the plastic flow varies with the angle  $\alpha$  around the sheet, giving rise to the formation of an undulating rim with a number of high points, known as “ears”, and an equal number of low points, called “troughs” (e.g. [1-3]). The characteristic earing profiles of deep drawn cups form because the sheet texture gives rise to different radial elongations in different in-plane directions of the blank. As shown on Fig. 2, for many commercially processed Al sheets the number of ears and troughs is four, and these are often situated under angles  $\alpha$  of  $0^\circ$  and  $90^\circ$  to the rolling direction – usually observed in soft, recrystallized sheet – or at the four positions  $\pm 45^\circ$  from the rolling direction, which is characteristic of the hard, as-rolled state. For many packaging applications material with low anisotropy, especially, low earing tendency, is required, however. Thus, the texture must be controlled in a way that earing is minimized.

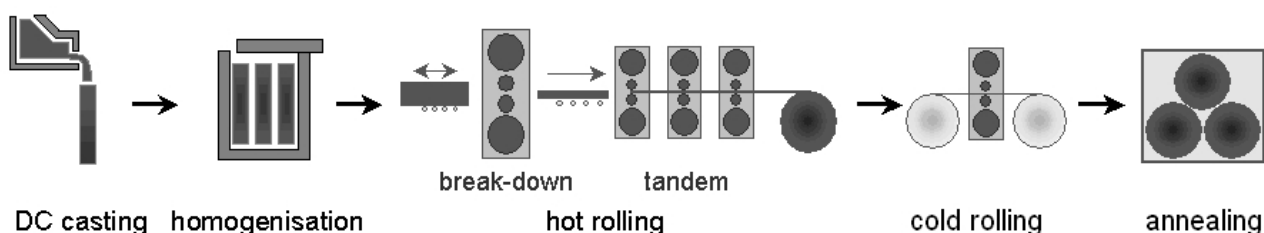


**Fig. 1.** Typical processing steps involved in the thermo-mechanical production of Al sheet.

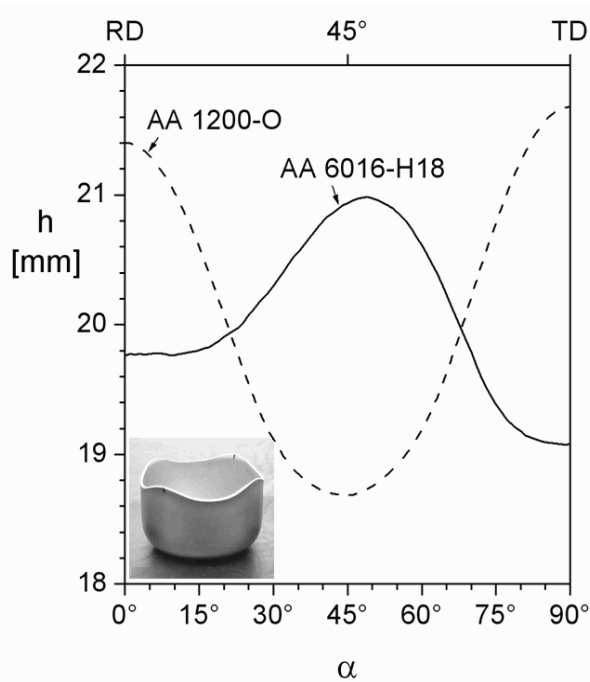


**Fig. 2.** Characteristic four-ear profiles (symmetrized) of Al sheet products: recrystallized AA 1200-O with  $0^\circ/90^\circ$  ears and cold rolled AA 6016-H18 with  $\pm 45^\circ$  earing.

In the present paper it is demonstrated how texture control can be applied during industrial processing of Al sheet so as to improve texture-related properties through the interplay of rolling and recrystallization with the resulting textural effects. Furthermore, we will describe simulation tools required for a through-process simulation of the development of microstructure, texture and resulting properties during the thermo-mechanical processing of Al sheet products. For that purpose, we combine an analytical softening model *AlSoft* with the rolling texture model *GIA* to simulate texture evolution during deformation, and with a model designated *ClaNG* treating the changes in microchemistry, i.e. variation in solute level and precipitation, during thermo-mechanical processing. The resulting anisotropic properties – here, earing – are simulated with a visco-plastic polycrystal-plasticity model *VPSC*. Eventually, a comprehensive through-process simulation of texture and texture-related properties will help to improve the resulting final-gauge material properties of Al sheet.

## 2. Simulation tools

### 2.1. Microchemistry Simulation

Through-process microstructure simulation requires information about the state of the material with regard to its local chemistry, which is usually referred to as “microchemistry”. Nowadays a broad thermodynamic database is available to compute phase diagrams based on the well-known CALPHAD approach (*Calculation of Phase Diagrams*). For Al alloys many of the required data have been determined in the framework of the European research programme COST 507 [4]. One of the most sophisticated data bases available – including the 15 most common elements of wrought Al alloys (Al-B-C-Cr-Cu-Fe-Mg-Mn-Ni-Si-Sr-Ti-V-Zn-Zr) and capable of handling quaternary phases like  $\alpha\text{-Al}_{15}(\text{Fe},\text{Mn})_3\text{Si}_2$  – is distributed commercially by *ThermoTech* [5].

The evolution in microchemistry, i.e. variation in solute level and precipitation, during thermo-mechanical processing has been calculated with a newly developed precipitation model, *ClaNG*, which is based on the *Classical Becker-Döring* theory for *Nucleation and Growth* of precipitates. A numerical implementation of this theory has the advantage that full size distributions can be tackled. The main improvement of the *ClaNG* model over former approaches is the introduction of multi-component thermodynamics into a kinetics model through the programming library *ChemApp*. Chemical driving forces and equilibrium composition of the various phases are derived by calls to *ChemApp* and the thermodynamic database *ThermoTech*. The only parameters that are known only imprecisely are the interfacial energies. Hence, interfacial energies of the relevant phases were determined by inverse modelling of a set of simple model alloys with systematic variation of the composition. Finally the equations for single nuclei are combined through the continuity equation and, therefore, entire size distributions of multi-component, multi-phase systems can be modelled. A more detailed description of the *ClaNG* model can be found in Refs. [6,7].

## 2.2. Simulation of rolling textures

The texture evolution accompanying rolling is routinely modelled with the help of Taylor-type deformation models. In such approaches the individual crystallites are assumed to deform by slip on a number of crystallographic slip systems so as to accommodate the prescribed macroscopic strain rate  $D_{ij}$ . For tandem hot rolling and, especially, for cold rolling of thin strip, the deformation is usually approximated by a plane strain state, where  $D_{11} = -D_{33}$  and all other strain rate components are assumed to be zero.

In the present study, we use the grain interaction (*GIA*) model [8] for simulating rolling textures. Unlike the above-mentioned conventional 1-point approaches, the *GIA*-model considers the deformation of an aggregate of eight brick-shaped grains embedded in a homogeneous surrounding. While the deformation of the whole aggregate is fully prescribed, a compatible relaxation of the deformation of the individual grains within the aggregate is possible. The remaining misfits are accommodated by a simplified arrangement of geometrically necessary dislocations (GND). The amount of relaxation of the shears, the slip rates and, ultimately, the grain reorientation is derived from a minimization of the total plastic work due to slip of the eight grains plus the energy introduced by the GNDs. In combination with random perturbations of the overall plane strain state and consideration of material parameters (work hardening and grain size), the *GIA* model has proven to be able to simulate the rolling textures of Al alloys with high accuracy [9].

## 2.3. Simulation of recovery and recrystallization

The softening behaviour – both recovery and recrystallization, including the related texture changes – can be simulated with the analytical softening model *AlSoft* [10,11]. This model is based on a two-parameter description of the microstructure of the as-deformed or recovered state, which is composed of subgrains with average size  $\delta$  and dislocations in the subgrain interior with density  $\rho$ . Recovery is assumed to be controlled by solute drag, where the rate-controlling mechanism is given by the thermal activation of the alloy elements in solid solution. During recovery, the increase in subgrain size and decrease in dislocation density as a function of time,  $t$ , and temperature,  $T$ , is described by the following differential equations:

$$\dot{\rho} = -\nu_D b B_\rho \rho^{3/2} D_0 \cdot \exp\left(-\frac{U_{RV}}{kT}\right) \cdot 2 \cdot \sinh\left(\frac{A_\rho \mu b^4 \sqrt{\rho}}{kT}\right) \quad \text{with } A_\rho = \omega_\rho c_{ss}^{-2/3} \quad (1)$$

$$\dot{\delta} = \nu_D b B_\delta D_0 \cdot \exp\left(-\frac{U_{RV}}{kT}\right) \cdot 2 \cdot \sinh\left(\frac{A_\delta \mu b^4}{\delta kT}\right) \quad \text{with } A_\delta = \omega_\delta c_{ss}^{-2/3} \quad (2)$$

( $\nu_D$ : Debye frequency,  $U_{RV}$ : activation energy,  $D_0$ : pre-exponential factor for diffusion of solids,  $k$ : Boltzmann constant,  $c_{ss}$ : concentration of solutes,  $B_i$  and  $\omega_i$ : alloy-specific constants).

The recrystallization model is an extension of the classical Johnson-Mehl-Avrami-Kolmogorov (*JMAK*) approach, treating recrystallization as a nucleation and growth process:

$$\dot{X} = (1 - X(t)) \cdot N(t) \cdot 4\pi \cdot r(t)^2 \cdot G(t). \quad (3)$$

The derivation of the density of recrystallization nuclei,  $N(t)$ , as well as simulation of the resulting recrystallization textures, has already been discussed in detail earlier [12,13]. The size of the nuclei,  $r(t)$ , is linked to their growth rate,  $G(t)$ , through

$$\dot{r} = G(t), \quad (4)$$

where the latter can be expressed through the well-known relation

$$G(t) = m(t) \cdot (p_D(t) - p_Z(t)). \quad (5)$$

Here,  $m(t)$  is the grain boundary mobility,  $p_D$  is the driving force for recrystallization due to dislocations and subgrains (see above), and  $p_Z$  is the back-driving force due to finely dispersed

particles (“Zener-drag”). Note that the required microchemistry data, including the particle density entering in the Zener-drag  $p_z$  as well as the concentration of solids  $c_{ss}$ , can be provided by the microchemistry model tool *ClanG*. In addition to providing the microstructural changes during recovery and recrystallization in terms of changes in dislocation density and subgrain size, the *AlSoft* model provides the flow stress  $\sigma$ , recrystallized volume fraction  $X(t)$ , grain size  $D_{RX}$  and texture changes upon recrystallization.

The recrystallization model is governed by four differential equations (Eqs. 1–4), which are solved for a given cycle of time,  $t$ , and temperature,  $T$ , by numerical routines with an adaptive step size control. For simulation of isothermal annealing  $T$  is set to the annealing temperature, while  $t$  increases up to the total heating time. For simulation of batch annealing  $T$  rises from the starting temperature  $T_0$  according to  $T(t) = T_0 + \dot{T} \cdot t$ , where  $\dot{T}$  represents the heating rate. Cooling of hot strip is simulated by a decrease of  $T$  from the coiling temperature down to ambient temperature with a negative  $\dot{T}$ .

## 2.4. Polycrystal-plasticity modelling of earing profiles

Simulation of texture-induced anisotropy – here, earing during cup deep drawing – can be performed with the visco-plastic self-consistent (VPSC) polycrystal-plasticity model developed by Lebensohn and Tomé [14]. In order to derive the boundary conditions for the VPSC computations, the evolution of stresses and strains operating during cup deep drawing was studied by detailed FEM analysis [15]. These FEM simulations have shown that plastic flow and, therefore, the formation of ears and troughs is concentrated in the flange of the blank under the blank-holder. In the flange a plane stress state prevails, in that the material is exposed to a tensile stress  $\sigma_r$  in the radial direction and a compressive stress  $\sigma_t$  in the tangential direction (Fig. 3). The stress in the through-thickness direction  $\sigma_z$  as well as the off-diagonal shear stresses  $\sigma_{rt}$  are almost zero. This stress state generates a positive radial strain rate  $D_r$  and a negative tangential strain rate  $D_t$ , while the through-thickness strain rate  $D_z$  is not necessarily zero. Thus, under making use of a feature of the VPSC model which permits enforcing mixed displacement/stress boundary conditions on the polycrystalline aggregate, the following load case is imposed to simulate earing:

$$D_{ij} = \begin{pmatrix} * & 0 & 0 \\ 0 & -1 & 0 \\ 0 & 0 & * \end{pmatrix} \cdot \dot{\epsilon} \quad \sigma_{ij} = \begin{pmatrix} \sigma_r & * & * \\ * & * & * \\ * & * & \sigma_z = 0 \end{pmatrix} \quad (6)$$

The asterisks \* indicate that the corresponding value is not prescribed;  $\dot{\epsilon}$  is a scalar measure of the strain rate [ $s^{-1}$ ]. It is seen that the stress components  $\sigma_r$  and  $\sigma_z$  are prescribed rather than the corresponding strain rate components  $D_r$  and  $D_z$ . All simulations in this study were performed with a non-zero radial stress of  $\sigma_r = -0.25 \cdot \sigma_t$  (see Ref. [16]).

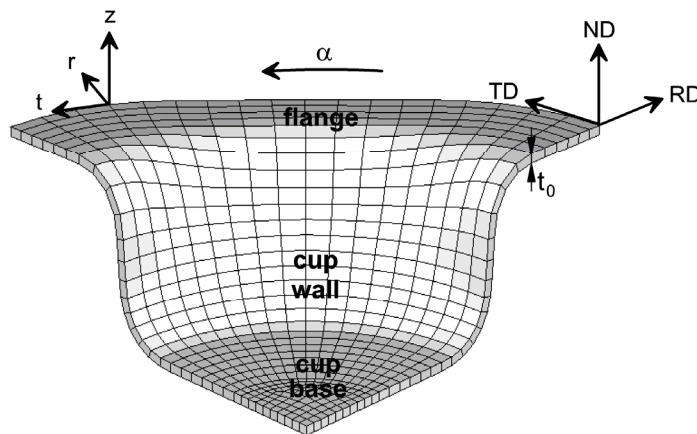


**Fig. 3.** Scheme illustrating the geometry of cup deep drawing used in this study.

Eq. (6) is expressed in the frame defined by radial direction,  $r$ , tangential direction,  $t$ , and through-thickness direction,  $z$ . This frame is related to the standard rolling frame  $\{RD, TD, ND\}$  through a rotation by angle  $\alpha$  about the common direction  $z = ND$  (Fig. 3). Thus, in order to derive the earing tendency under a given angle  $\alpha$ , the strain in radial direction is determined for the texture in this particular position of the blank. For this purpose, the strain and stress tensors are

rotated by  $\Delta\alpha$  in steps of typically  $5^\circ$  about  $z$ . Then, the earing profile along the rim of a deep-drawn cup is given by the radial strain rate  $D_r$  or, more precisely, by the normalized strain rate ratio  $q = D_r/D_t$  as a function of  $\alpha$ . The absolute height of a deep-drawn cup is controlled by the radii of initial blank,  $r_B$ , and punch,  $r_P$ , and, to a lesser extent, by sheet thickness,  $t_0$ , and the radius of the punch profile,  $r_{pp}$ . As detailed in Ref. [17], the exact cup height profile  $h$  can then be computed from the strain rate ratio  $q$  as a function of the in-plane angle  $\alpha$  from

$$h(\alpha) = t_0 + (1 - \pi/4)(2r_{pp} + t_0) + \frac{r_B^{q+1} - (r_P + t_0)^{q+1}}{(q+1)(r_P + t_0/2)^q}. \quad (7)$$

### 3. Application example – texture and anisotropy in AlMnMg 3xxx packaging alloys

For many packaging applications material with low anisotropy, especially, low earing tendency, is required. Thus, the texture must be controlled in a way that earing is minimized. In principle, zero earing may be attained either by a random texture or by a texture comprised of uniform intensities around the sheet normal direction, with the latter being readily accomplished by way of the typical  $\{111\}$ //ND  $\gamma$ -fibre texture of deep-drawing steels. In Al alloys, in contrast, both texture types are not easily obtained. Rather, earing is controlled by means of producing mixed textures comprising both rolling and recrystallization texture components. That is to say, the resulting  $0^\circ/90^\circ$  and  $\pm 45^\circ$  earing behaviour is superimposed, which results in a balanced earing profile with reduced anisotropy.

Accordingly, partially recrystallized strip showing a mixed rolling and recrystallization texture may be well suited for forming operations that mandate low earing (e.g. [18]). However, back-annealing cannot generally be used to moderate earing, which is usually due to the insufficient mechanical strength of the partially recrystallized state (H2x).

The most well-known example of the use of mixed textures applies to the production of can body stock from alloy AA 3104 (Fig. 4). For aluminium beverage cans highly cold rolled states (H19) are used to meet the strength requirements ( $>275$  MPa). Thus the sheets always comprise a strong  $\beta$ -fibre rolling texture accompanied by the formation of  $45^\circ$  ears. These  $45^\circ$  ears are balanced by a cube texture which is retained from the recrystallized hot strip. Due to the slow rotation rate of the cube orientation the resultant  $0^\circ/90^\circ$  ears countervail the newly forming  $45^\circ$  ears up to rather high rolling reductions [19]. Thus, the formation of a

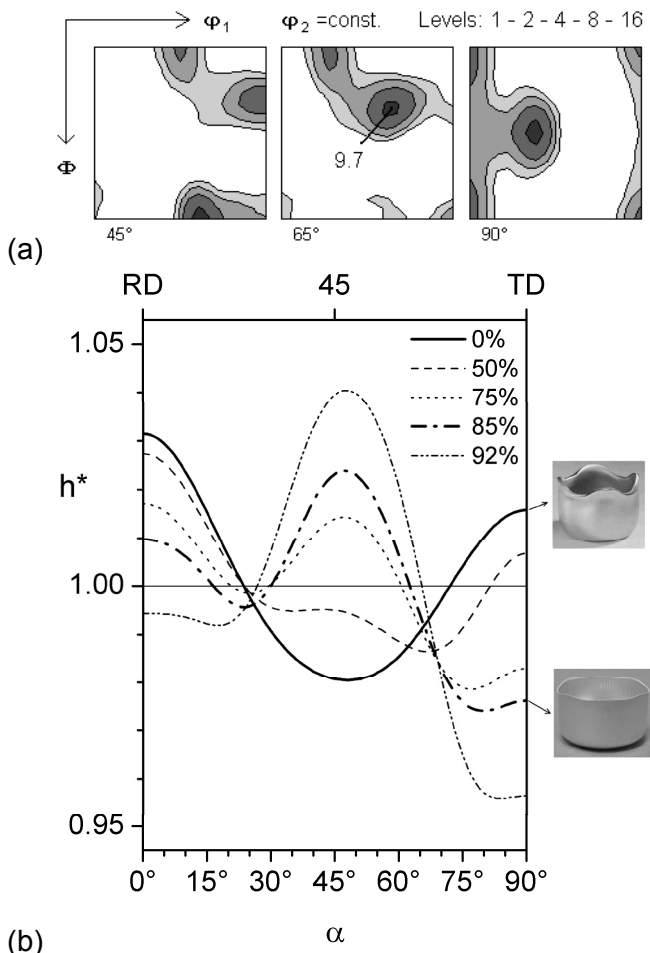


**Fig. 4.** Correlation of texture and earing in AA 3104 can body stock. (a) texture at final gauge (H19), showing a rolling texture superimposed on a cube texture retained from the recrystallized hot strip (ODF  $\phi_2 = 45^\circ$ ,  $65^\circ$  and  $90^\circ$  sections), (b) evolution of earing profiles with increasing rolling strain, showing transition from  $0^\circ/90^\circ$  earing towards weak earing with mixed  $0^\circ/90^\circ$  and  $45^\circ$  ears.

suited rolling texture with minimum earing requires the optimum combination of the strength of cube texture in the initial hot band as well as amount of subsequent cold rolling, which is typically about 85% for fully recrystallized AA 3104 hot strip. Fig. 4a shows the resulting texture, which consists of a mixture of the cube texture retained from the recrystallized hot strip and the newly formed  $\beta$ -fibre rolling texture components. The resulting cup height profile – revealing a characteristic six-ear profile with ears under  $0^\circ$ ,  $45^\circ$ ,  $135^\circ$ ,  $180^\circ$ ,  $225^\circ$  and  $315^\circ$  to the rolling direction (Fig. 4b) – is generally deemed suitable for production of Al beverage cans.

Figs. 5 and 6 pertain to another example of 3xxx packaging products requiring minimum earing, yet at lower strength levels (typically H14 or H16). Here, texture and earing are controlled through an intermediate annealing before the final rolling pass (e.g. [20,21]). Fig. 5 shows a sequence of textures along the process chain of laboratory cold rolled AA 3105 (AlMn0.5Mg0.5) which is used e.g. for screw caps of pressurized bottles. The (fully recrystallized) hot strip reveals a sharp cube texture and, accordingly, pronounced  $0^\circ/90^\circ$  earing (Fig. 6). Rolling to intermediate gauge leads to formation of a  $\beta$ -fibre rolling texture together with an appreciable increase of  $45^\circ$  earing. Upon inter-annealing the material recrystallizes under formation of a cube recrystallization texture with medium intensities of the R orientation. This texture is characterized by a typical eight-ear profile with ears under  $0^\circ$ ,  $45^\circ$  and  $90^\circ$ . Final gauge properties are achieved through a final rolling pass to medium strength (H16).

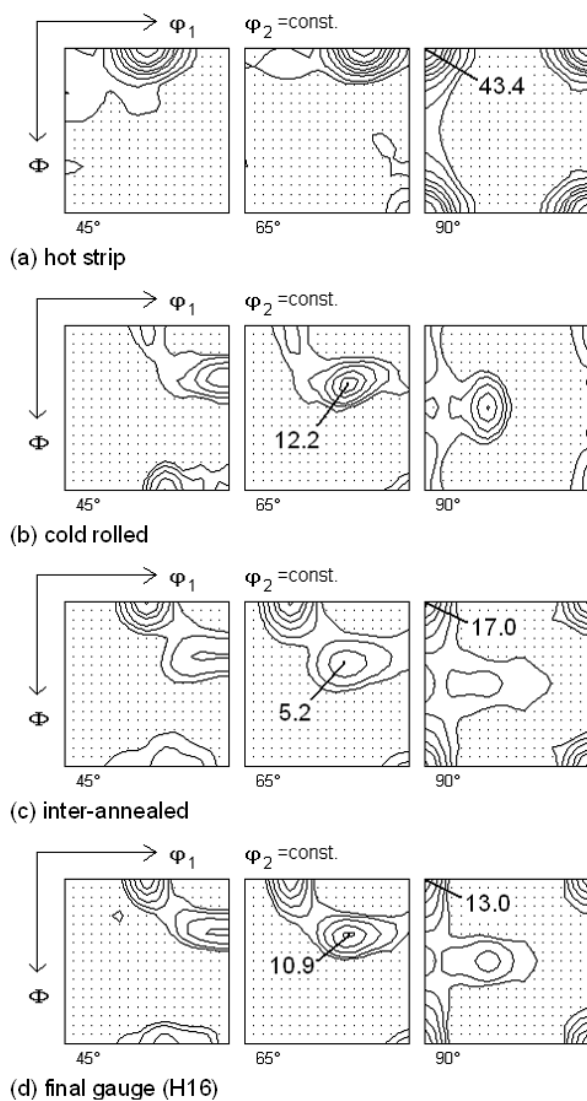


**Fig. 5.** Evolution of texture along the process chain of laboratory cold rolled AA 3105.

This light rolling pass of the order of 20-30% thickness reduction – sometimes called temper rolling – sharpens the rolling texture orientations at the expenses of the cube component, yet the rolling reduction is evidently not large enough so as to significantly degrade the latter. Accordingly, the final gauge H16 material comprises balanced cube and rolling texture orientations and, in consequence, the desired light earing profile suitable for products requiring minimum earing properties.

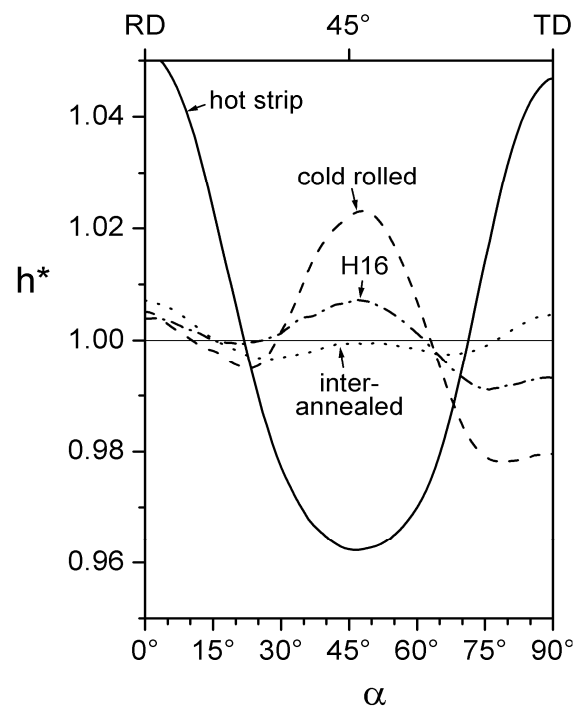


**Fig. 6.** Evolution of earing profiles along the process chain of laboratory cold rolled AA 3105.

#### 4. Summary

In the field of aluminium alloys, texture investigations are of great importance since texture affects a number of materials properties, which are important for practical applications of Al sheet products. The evolution of texture and texture-related properties is strongly influenced by the various steps of thermo-mechanical processing of Al sheets – homogenization, hot and cold rolling and possible intermediate and/or final annealing. In the present paper it is demonstrated how texture control can be applied during industrial processing of Al sheet so as to minimize earing through the interplay of rolling and recrystallization with the resulting textural effects. Accordingly, a comprehensive through-process simulation of texture and texture-related properties during the thermo-mechanical processing of Al sheet products will help to improve the resulting final-gauge material properties of Al sheet. The development of a through-process model of microstructure and texture evolution necessitates coupling of models for simulating the evolution of microstructure, microchemistry and crystallographic texture during the various processing steps involved.

#### References

- [1] J.C. Blade, J. Austr. Inst. Metals 12 (1967) 55.
- [2] W.B. Hutchinson, A. Oscarsson, Å. Karlsson, Mater. Sci. Tech. 5 (1989) 1118.
- [3] O. Engler, J. Hirsch: Mater. Sci. Eng. A452-453 (2007) 640.
- [4] I. Ansara, A.T. Dinsdale and M.H. Rand: *Thermochemical Database for Light Metal Alloys (Final Report COST 507 V2)*, European Commission, Brussels 1998).
- [5] N. Saunders: J. Japanese Inst. Light Metals 51 (2001) 141.
- [6] M. Schneider, G. Gottstein, L. Löchte and J. Hirsch: Mater. Sci. Forum 396-402 (2002) 637.
- [7] G. Gottstein, M. Schneider and L. Löchte: in *Proc. ICAA 9*, eds. J.F. Nie, A.J. Morton and B.C. Muddle (Inst. Mater. Eng. Australasia Ltd., 2004) pp. 1116.
- [8] M. Crumbach, G. Pomana, P. Wagner and G. Gottstein: in *Proc. 1<sup>st</sup> Joint Int. Conf. on Recrystallization and Grain Growth*, eds. G. Gottstein, D.A. Molodov (Springer-Verlag, Berlin, 2001) pp. 1053.
- [9] O. Engler, M. Crumbach and S. Li: Acta Mater. 53 (2005) 2241.
- [10] H.E. Vatne, K. Marthinsen, R. Ørsund and E. Nes: Metall. Trans. 27A (1996) 4133.
- [11] J.A. Sæter, B. Forbord, H.E. Vatne and E. Nes: in *Proc. ICAA6*, eds. T. Sato et al. (JILM, Japan, 1998) pp. 113.
- [12] H.E. Vatne, T. Furu, R. Ørsund and E. Nes: Acta Mater. 44 (1996) 4463.
- [13] O. Engler: Textures and Microstr. 32 (1999) 197.
- [14] R.A. Lebensohn and C.N. Tomé: Acta Metall. Mater. 41 (1993) 2611.
- [15] O. Engler and S. Kalz: Mater. Sci. Eng. A373 (2004) 350.
- [16] P. Van Houtte, G. Cauwenberg and E. Aernoudt: Mater. Sci. Eng. 95 (1987) 115.
- [17] R. Schouwenaars, P. Van Houtte, A. Van Bael, J. Winters and K. Mols: Text. Microstr. 26-27 (1996) 553.
- [18] J. Hirsch and O. Engler: in *Proc. 1<sup>st</sup> Joint Int. Conf. on Recrystallization and Grain Growth*, eds. G. Gottstein, D.A. Molodov (Springer-Verlag, Berlin, 2001) pp. 731.
- [19] O. Engler, L. Löchte and J. Hirsch: Acta Mater. 55 (2007) 5449.
- [20] S.E. Naess: Z. Metallkd. 82 (1991) 259.
- [21] O. Engler and J. Hirsch: Inter. J. Mater. Res. 100 (2009) 564.